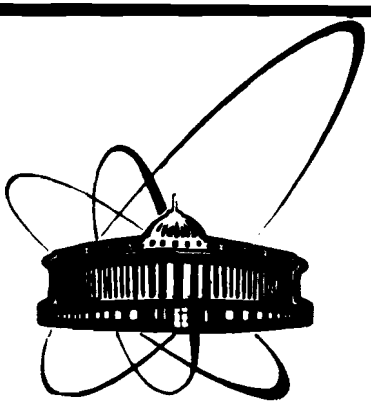

объединенный
институт
ядерных
исследований
дубна

E7-89-680

D.D.Bogdanov, A.M.Rodin, S.I.Sidorchuk,
S.V.Stepantsov, G.M.Ter-Akopian, V.A.Timakov

STUDY OF THE ION-OPTICAL PROPERTIES OF THE MASS-SPECTROMETER LIDIA

Submitted to "Nuclear Instruments and Methods"

1989

1. INTRODUCTION

The ultrasensitive mass-spectrometer LIDIA was designed [1] to develop a novel instrumental approach to the search for superheavy elements in natural samples (see reviews [2,3]). This type of mass-spectrometer can also be useful for the local analysis of the elemental composition of rocks, minerals and synthetic pure materials.

The purpose of the LIDIA design is to reach a sufficient sensitivity for determining concentrations of 10^{-14} at./at. for heavy element content in a sample of basically light elements. With the absolute sensitivity of 10^{6} atoms of the element under study the minimum weight of the specimen will be about 10 mg. Therefore the operation regime of the mass-spectrometer was chosen so as to achieve the comparatively high efficiency of using the specimen material, namely, to register in the focal plane 10^{-6}–10^{-3} of the number of the specimen atoms. This, of course, resulted in the reduction of the instrumental mass resolution to the rather low value of $m/\Delta m \leqslant 300$. The poor resolution and the low detection limit entailed the necessity of taking special measures to suppress the background from molecular ions and scattered ions of the most intensive mass lines. These two sources of the background usually limit the sensitivity of mass-spectrometric analysis.

The distinguishing feature of a laser-produced plasma ion source is the possibility of considerable suppression of the molecular ion background. This kind of ion source capable of making the chemically non-selective analysis of specimens, which provides a very low background from molecular ions was described in papers [4,5]. In the source the flux of molecular ions did not exceed 10^{-6} of the total number of ions in the ion beam. An additional reduction of this background can apparently be achieved by separating doubly- and triply-charged ions from the laser plasma, by their charge exchange on the gas target and by performing the mass-spectrometric analysis of the ions that underwent the charge exchange $2^{+} \rightarrow 1^{+}$ or $3^{+} \rightarrow 1^{+}$ (ref. [6]).

To suppress the background due to the scattered ions the mass-spectrometer should provide the two- or three-stage selection of the mass lines of the heavy elements searched for. The necessity of obtaining a certain efficiency of specimen utilization together with the specific features of the laser source (high density and high temperature of plasma, the great space charge of the beam) led to the choice of rather large size system and imposed a limitation on the minimum value of its acceptance.

The present paper gives a brief description of the ion-optical scheme of the mass-spectrometer, its design features and the results of the experiments aimed at tracing α-particle beams. For details the reader is referred to papers [7,8].

2. LAYOUT OF THE FACILITY

The mass-spectrometer is shown schematically in fig.1.

Two dipole magnets M1 and M2 and four quadrupole magnetic lenses Q1-Q4 make up an achromatic mirror-symmetric system with an intermediate image 0_2. The main purpose of the system is to transform the mass-spectrometer source from the position 0_1 to the position 0_3, and to pick out from the whole mass-spectrum of the ion beam the mass range determined by the momentum acceptance of the facility. Herewith, the mirror-symmetry condition is achieved by the corresponding excitation of the quadrupoles Q1-Q4 and the surface current coils (α-coils). The latter create magnetic field regions with quadrupole components in the dipole magnets M1-M2.

The dipole magnet M3 and the quadrupole lens Q5 produce, in the focal plane 0_4, the image of the mass lines that have passed through the achromatic system.

The width and shape of the mass line in the achromatic image plane 0_3 are mainly influenced by the aberration $x/x'\delta$ (from now on TRANSPORT notations [9] are used). To eliminate this effect sextupole

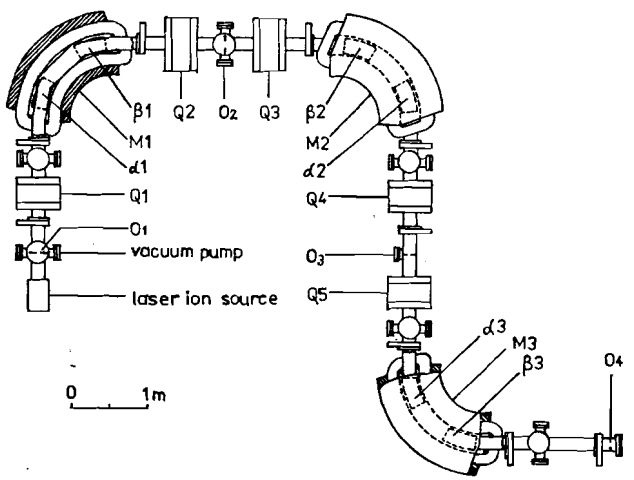

Fig. 1. Schematic layout of the LIDIA mass-spectrometer.

components of the magnetic fields are provided in the magnets M1 and M2 by surface current coils of different kinds (ß-coils).

The most important aberrations in the focal plane 0_4 are $x/x'\delta$ and x/x'^2. To compensate for them the pole profiles at the sides of the magnet M3 are curved, namely: at entrance-convex (R=0.696 m) and at exit-concave (R=0.551 m). Here, too, for flexibility in the tuning of the mass-spectrometer the surface coils of α- and ß-types are mounted.

The mass resolution in the plane of the intermediate image 0_2 is strongly limited by the presence of a large uncompensated geometrical aberration x/x'^2 and does not exceed $m/\Delta m \leq 100$.

The main ion-optical parameters of the mass-spectrometer are given in table 1. The technical characteristics and magnetic fields for the case when the facility is tuned to the momentum p=237 MeV/c are listed in table 2. This momentum would be obtained, e.g., by the single-charged ions with mass 300 a.m.u. accelerated to an energy of 100 keV. The first order sine- and cosine-like trajectories are shown in fig.2. In fig.3 one can see the beam envelopes calculated for the source size 2x2 mm², the angular divergence $\pm$17.5 mrad both horizontally and vertically, and momentum spread $\pm$2.5%. Fig.4 shows the calculated space and momentum acceptances of the mass-spectrometer.

The estimated mass-spectrum in the vicinity of the mass m=300 a.m.u. in the focal plane 0_4 is shown in fig.5. The calculation was made without energy spread of the ions. This allowed one to estimate the maximum resolving power of the facility. It turned out to be $(m/\Delta m)_{max} \simeq 330$ (10%-level) in the focal plane 0_4 and $(m/\Delta m)_{max} \simeq 90$ (10%-level) in the intermediate one, 0_2. Fig. 6 illustrates the one-dimensional mass spectra calculated without (top part) and with (bottom part) energy spread.

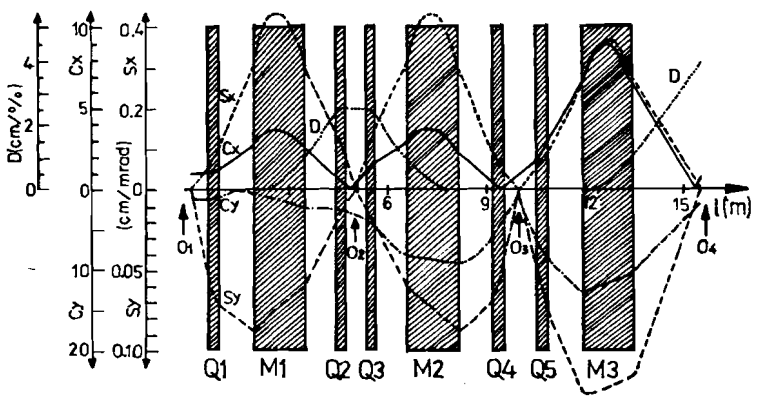

Fig. 2. The first-order characteristic functions of the mass-spectrometer in TRANSPORT notations.

For the latter ΔE=0.1 keV ($\Delta E/E$=0.2% for E=50 keV) which is typical for the laser plasma ion source[6]. One can see the remarkable decrease in the resolving power (e.g., for the focal plane 0_4 $m/\Delta m \leq 165$). Nevertheless, it is still suited for our task.

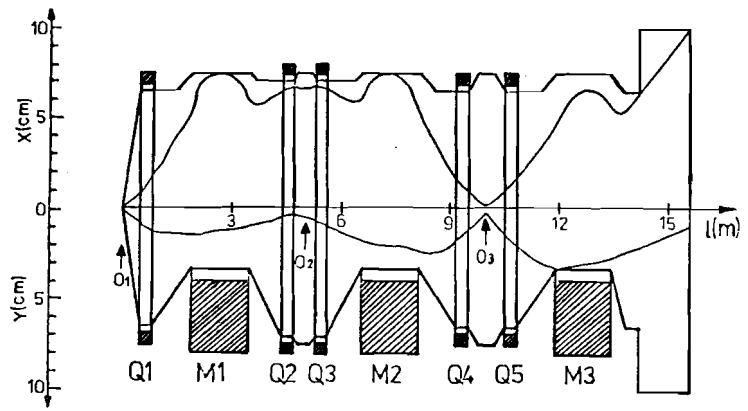

Fig. 3. The calculated beam envelopes through the mass-spectrometer.

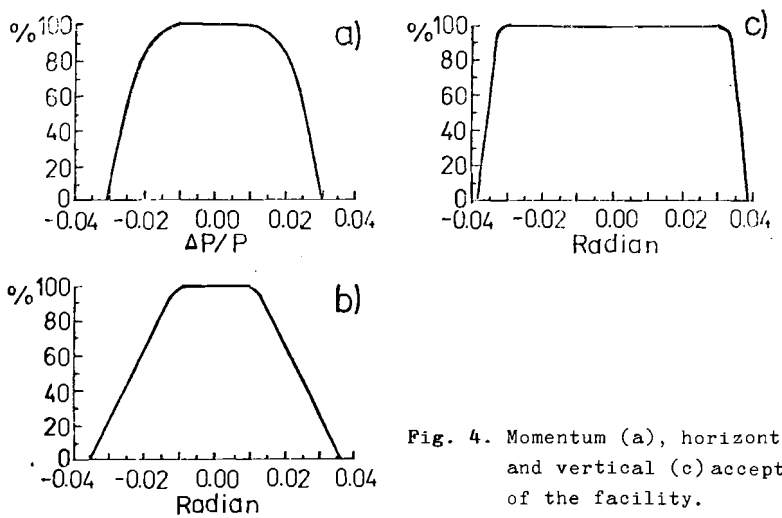

Fig. 4. Momentum (a), horizontal (b) and vertical (c) acceptances of the facility.

Table 1. Specifications of the mass-spectrometer

Solid angle	2.3 msr
Momentum acceptance	$\pm$2.5%
Mass resolution (10%-level)	330
Momentum range	60-390 MeV/c
Dispersion along focal plane	4.0 cm/%(Δp/p)
Dispersion along intermediate focal plane	2.5 cm/%(Δp/p)
Focal plane tilt angle	85°
Intermediate focal plane tilt angle	90°
Dispersion plane	Horizontal
Total path length	15.5 m

Table 2. First and second order TRANSPORT input parameters for the mass-spectrometer

Source slit (0_1)			p=237 MeV/c
Drift	0.517 m		
Quad (Q1)	l_{eff}=0.348 m	g=-306 G/cm	R_0=6.93 cm
Drift	1.067 m		
Dipole (M1)	$\tau_{entr.}=\tau_{exit}=21.5^0$	$\phi=90^0$	ρ=1.0 m
	B_0=7.903 kG	α=-0.0151	β=1.86
Drift	0.95 m		
Quad (Q2)	$l_{eff.}$=0.3141 m	g=145 G/cm	R_0=7.5 cm
Drift	0.35 m		
Intermediate focal plane (0_2)			
Drift	0.35 m		
Quad (Q3)	$l_{eff.}$=0.3141 m	g=145 G/cm	R_0=7.5 cm
Drift	0.95 m		
Dipole (M2)	$\tau_{entr.}=\tau_{exit}=21.5^0$	$\phi=90^0$	ρ=1.0 m
	B_0=7.903 kG	α=-0.0151	β=1.86
Drift	1.067 m		
Quad (Q4)	$l_{eff.}$=0.348 m	g=-306 G/cm	R_0=6.93 cm
Drift	0.517 m		
Achromatic focus plane (0_3)			
Drift	0.5 m		
Quad (Q5)	$l_{eff.}$=0.348 m	g=-185 G/cm	R_0=6.93 cm
Drift	1.067 m		
Dipole (M3)	$\tau_{entr.}=\tau_{exit}=21.5^0$	$\phi=90^0$	ρ=1.0 m
	B_0=7.903 kG	α=0.167	β=0.0
	$R_{entr.}$=0.696 m	R_{exit}=-0.551 m	
Drift	2.095 m		
Focal plane (0_4)			

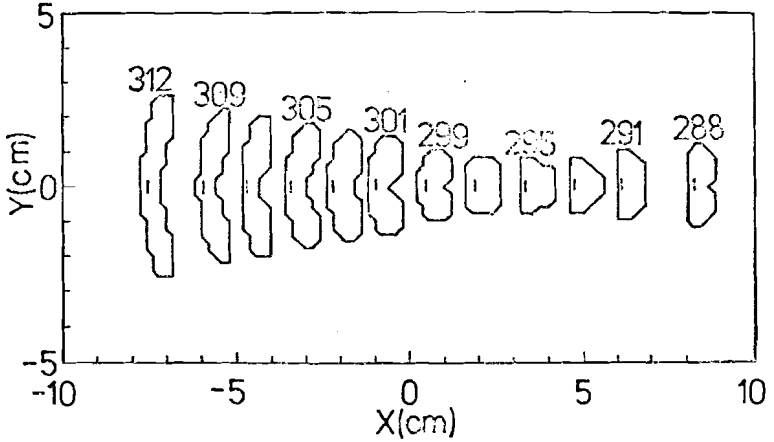

Fig. 5. Two-dimensional mass-spectrum in the focal plane 0_4 calculated for the mass range near the m=300 a.m.u. ($x_0=y_0=\pm 1.0$ mm, $x_0'=Y_0'=\pm 17.5$ mrad, $\Delta p/p=0.0$).

3. MASS-SPECTROMETER MAGNET DESIGN, PUMPING SYSTEM AND TOLERANCES

The industrial standard magnetic quadrupoles of two types Q1, Q4, Q5 and Q2, Q3 were chosen as the main focusing elements of the facility. Their basic ion-optical parameters are given in table 3. For the momentum dispersion of the ion beam three bending magnets were used whose characteristics are listed in table 4.

The maps of the magnetic fields of all these elements were carefully measured with scanning devices designed for these purposes and equipped with Hall probes. Within the accuracy of observation the effective lengths of the quadrupoles ($l_{eff.}$) turned out to be practically independent of the currents of excitations of the coils (see table 5). The Fourier analysis of the lens magnetic fields allowed one to determine the gradients (g), the shift of the ion-optical axes of the quadrupoles with respect to the geometrical ones in horizontal (Δx) and in vertical (Δy) directions, and the angle (γ) between the real and the geometrical quadrupole symmetry axes. All these values (except for

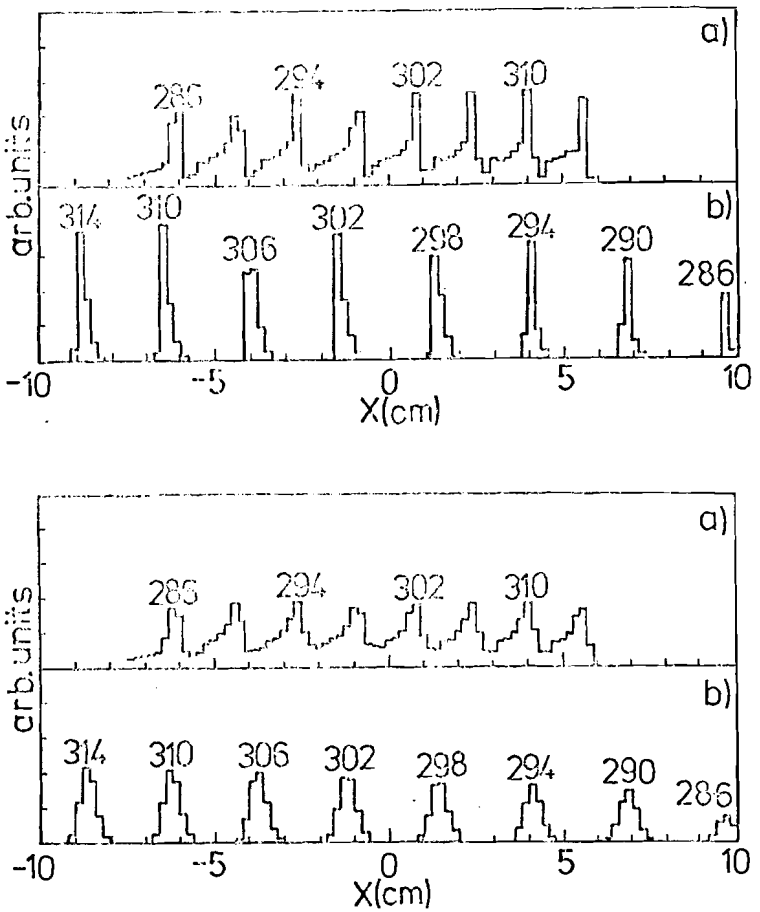

Fig. 6. One-dimensional mass spectra in the focal planes 0_2 (a) and 0_4 (b) at $\Delta p/p=0.0$ (top part) and $\Delta p/p=0.1\%$ (bottom part).

gradients) are weakly dependent on the coil excitation currents. In table 5 they are given at currents close to the maximum ones for each quadrupole. The last row in the table is the upper limit of the lens magnetic field sextupole constituence (B) normalized to the quadrupole

Table 3. Specifications of the magnetic quadrupoles

	Q1,Q4,Q5	Q2,Q3
1. Aperture diameter, mm	138,6	150
2. Maximum gradient, G/cm	420	800
3. Maximum current, A	I0.5	508
4. Length of the pole pieces, mm	300	250
5. Shape of the pole pieces	cylindrical (r=78 mm)	cylindrical (r=85 mm)

Table 4. Specifications of the dipole magnets

1. Maximum magnetic field	I.3 kG
2. Maximum current	470 A
3. Mean bending radius	I.0 m
4. Bending angle	90^0
5. Pole side tilt angles at entrance and exit	$2I.5^0$
6. Pole side curvature radius (only for magnet M3)	
at entrance (convex)	696 mm
at exit (concave)	55I mm
7. Magnetic road width ($\Delta B/B \leqslant 0.I\%$)	I30 mm
8. Magnetic gap	80 mm

Table 5. Some results of the Fourier analysis of the quadrupole magnetic fields

	Q1	Q4	Q5	Q2	Q3
Current, A	9.I	9.I	9.I	395	395
g, G/cm	377	379	372	748	723
$l_{eff.}$, mm	348	348	349	3I2	3I4
Δx, mm	-0.2	-0.6	-0.4	0.	0.3
Δy, mm	0.3	0.6	0.2	0.3	0.5
γ, degree	0.5	0.6	0.2	-I.4	-0.7
ß	$3\ I0^{-3}$	$3\ I0^{-3}$	$3\ I0^{-3}$	$2\ I0^{-3}$	$3\ I0^{-3}$

one at a given radius r_n=60 mm (α and ß in this work are dimensionless parameters, being deduced from the usual expansion of the magnetic field near the optical axis[9]).

The magnets M1 and M2 are practically identical and have a little positive sextupole component of the field due to the employed profile of the poles. The value of this component lies in the range ß=0.4–0.6 depending upon the excitation current. In the magnet M3 the sextupole term is absent within the accuracy of measurement.

The elements of fine tuning of the mass-spectrometer are the coils consisting of two sets of concentric copper conductors each mounted on a single insulated base, as described in ref.[10]. For the α-coil the widths of conductor bands are the same while for the ß-coil they linearly decrease in both directions from the central line of symmetry. Having been arranged in magnets as shown in figs.1 and 7, these sets create magnetic fields with linear (α-coil) and quadratic (ß-coil) dependency on the radius.

The desing of our coils permits operation with currents up to 100 A without remarkable heating of the insulation material which enables one to reach the field gradient value g_{max}=0.2 T/m (α_{max}=0.20) for the α-coil and the sextupole component value $ß_{max}$=1.8 for the ß-coil.

The stabilization system of the dipole and quadrupole magnet power supplies provides the current pulsation level of no more than 0.01% and

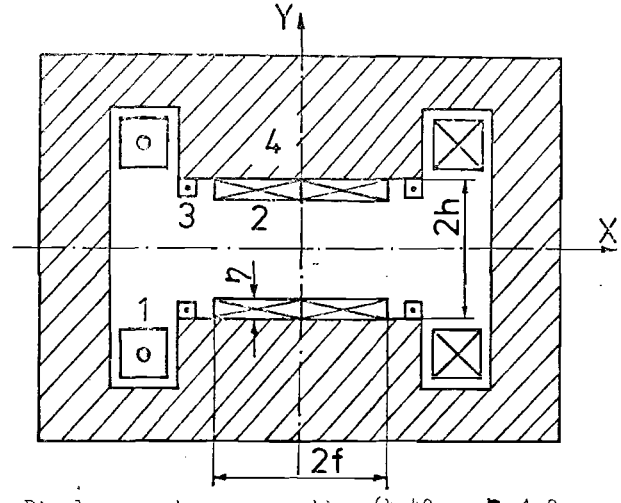

Fig. 7. Dipole magnet cross-section (h=40 mm, η=1.0 mm, f=60 mm): 1 – main winding ($I_0 \leqslant 470$ A); 2 – fine tuning correction coil (α-coil in this case) ($I_\alpha \leqslant 100$ A); 3 – return conductors of the correction coil; 4 – yoke of the magnet.

0.2%, respectively. As to the α- and ß-coils the inductive filters that were used for their power supply diminished the pulsations down to a value not exceeding 2% which is sufficient to work with since the needed field correction range is about 1-2%.

In the automatic mode the digital-analog-converters with computer control are used for the current setting. The accuracy of current setting is 0.1% for quadrupoles and 0.01% for dipoles.

The pumping system of the mass-spectrometer includes six units consisting of the sputter- and getter-ion-pumps with a pumping rate of 2000 l/sec. The volume of the getter-ion-pump is evacuated by a turbopump and is connected with the analyzing part through the differential step of evacuation. The analyzing part of the vacuum system is made with due regard to the demands of the high-vacuum technique and is intended to reach a vacuum below 10^{-9} torr.

The whole facility was assembled on a monolithic reinforced concrete plate with a thickness of 0.7 meter. The linear alignment accuracy of mounting the ion-optical elements was measured to be 0.3 mm horizontally, 0.1 mm vertically and 1.0 mm along the beam axis. The angular one was about 0.2 mrad. In the long run of the facility exploitation it was not necessary to make an additional correction of the magnetic element positions.

4. MEASUREMENT OF THE ION-OPTICAL PARAMETERS OF THE MASS-SPECTROMETER

The ion-optical characteristics of the mass-spectrometer in the positions 0_2, 0_3 and 0_4 (fig. 1) have been studied. For this purpose a ^{249}Cf α-source with a 9 mm diameter of the working surface was installed in the position 0_1 and covered by an 9 µm aluminium foil, so that the maximum of the α-particle spectrum was at the energy 3.95 MeV (FWHM=10%), which corresponds to the energy 50 keV and the momentum spread of $\pm$2.5% for singly charged ions with mass 78 a.m.m. The source dimensions were formed by means of a set of three windows made in the aluminium foils, namely, two round orifices with diameters of 3 mm and 6 mm and one rectangular orifice 3 mm wide and 9 mm high. The α-particle intensities for each of these cases and the diameters of diaphragms that determine the angular range of α-particles emitted from the source are given in table 6. In order to single out the momentum window of the particles two rectangular slits with dimensions 120x30mm² ($\Delta p/p=\pm 2.4\%$) and 80x30 mm² ($\Delta p/p=\pm 1.6\%$) were placed in the position 0_2. The α-particle counting was carried out with Si(Au) detectors. In all cases the experimental errors did not exceed $\pm$3%.

Table 6. Measured values of mass-spectrometer transmissions

Source size (0_1)	Ø3 mm				3x9 mm²	Ø6 mm
Source intensity (α/sec in 2π sr)	$1.54\ 10^6$				$4.05\ 10^6$	$4.86\ 10^6$
Size of the diaphragm installed at a distance of 390 mm from 0_1	Ø14 mm (1.0 msr)		Ø20 mm (1.5 msr)	14x28 mm² (2.3 msr)		
Momentum range	$\pm$2.4%	$\pm$1.6%				
Transmission (%) from the plane 0_1 to						
plane 0_2:	85	83	76	86	77	78
plane 0_3:	73	77	65	81	65	73
plane 0_4:	64	81	64	83	64	74
α-particle yield in the focal plane 0_4 (relative units)	1.1	1.0	1.5	2.1	5.1	7.0

The results of measuring the beam profiles along two transverse directions in the achromatic focus 0_3 are shown in fig.8. The source diameter and angular divergence along both transverse directions were 3 mm and $\pm$17.5 mrad, respectively. Three histograms (1,2,3) in the figure show the gradual improvement of the beam focussing that is reached (1) by means of proper tuning of the quadrupoles Q1-Q4,(2) by additional excitation of the α-coils, and (3) ß-coils. The solid lines in the figure are the profiles calculated for the same initial conditions. It is seen that the form of the beam along the vertical direction is practically not affected by the correction coils whereas the gradual increase of the histogram area is due to the finite width (10 mm) of the scanning slit along the horizontal direction.

The transmissions measured with various dimensions of the source, i.e., the ratios of the number of α-particles that reached the positions 0_2, 0_3 and 0_4 to their number emitted from the source 0_1 within some solid angle are presented in table 6. It is seen that the best values at a momentum acceptance of $\pm$1.6% were obtained for the source with a diameter of 3 mm and for two solid angles of $1\ 10^{-3}$ sr and $2.3\ 10^{-3}$ sr. It should also be noted that the main losses of the beam ($\simeq$15%) in these cases take place in the first magnet.

So, the transmission of the beam from the location 0_1 to the focal plane 0_4 could be assumed to be about 100% for the acceptances equal to

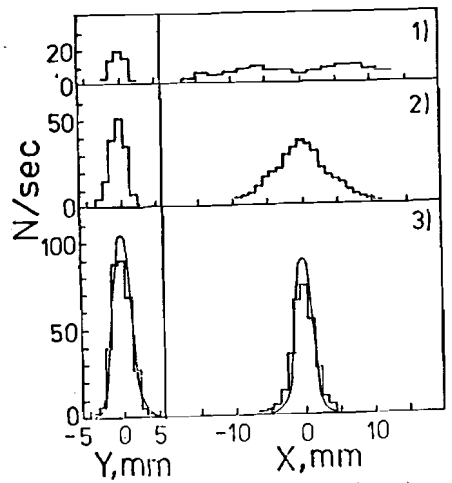

Fig. 8. The profiles of the beam along two transverse directions in the achromatic focus 0_3 after successive excitation of: 1 - quadrupoles Q1-Q4; 2 - α-coils; 3 - ß-coils.

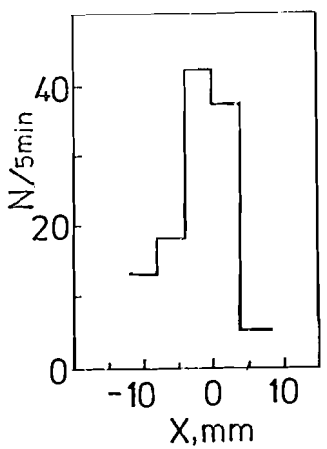

Fig. 9. The 4.7875 MeV line of the ^{226}Ra spectrometric α-source obtained in the focal plane 0_4 (source slit is 6x8 mm^2).

1.5x15π mm mrad (dispersive plane), 1.5x35π mm mrad (axial plane), and momentum acceptance $\pm$1.6%.

In terms of an increase in the efficiency of using the specimen material a big source diameter of 6 mm and a solid angle of 2.3 10^{-3}sr is to be of interest. The transmission in this case is not so poor (74%).

Another set of experiments has been devoted to measuring the momentum dispersions and resolving powers in the positions 0_2 and 0_4. In the experiments the ^{226}Ra spectrometric α-particle source with an intensity of 1 10^4 α/sec in 2π steradians was used. Its size was restricted to a spot with a diameter of 8 mm. The slit size, in front of the detector, was 10x30 mm^2 both in the positions 0_2 and 0_4.

By scanning the magnetic field of first (third) magnet and comparing the positions of the intensity maximum in two cases when the detector is on the optical axis and 30 mm apart one could determine the corresponding momentum dispersion. It turned out to be (24.9$\pm$0.6)mm/% (Δp/p) in the intermediate focus 0_2 and (40$\pm$1) mm/%(Δp/p) in the focal plane 0_4.

Fig. 9 shows the 4.7875 MeV line measured by the mechanical scanning of the 4 mm detector slit. It is seen that though the size of the source, 6x8 mm^2, is relatively big the resolution is still not too poor, m/Δm $\lesssim$270 (FWHM).

The estimate of the resolving power in the intermediate focus 0_2 with the source diameter of 3 mm has given m/Δm$\simeq$100 (FWHM).

5. CONCLUSION

In the present paper the results of the experiments aimed at forming the magnetic fields and the alignment of the mass-spectrometer ion-optical elements were described. The aberrations of up to the second order inclusively were taken into consideration. The measurements with α-particle sources showed that the space acceptance of the facility, its momentum dispersion and momentum acceptance, and the form of the achromatic image are in good accord with the calculated ones.

The mass-spectrometer is made operational with a laser ion source.

The authors would like to express their gratitude to Academician G.N.Flerov for his permanent interest in this work, Yu.V.Grigoriev for his help during the operation of the mass-spectrometer and V.A.Baranov for his assistance in providing the computer software.

REFERENCES

1. G.M.Ter-Akopian et al., JINR, E13-82-639, Dubna, 1982.
2. G.N.Flerov, G.M.Ter-Akopian.-In: Treatise on Heavy Ion Science, edited by D.Allan Bromley, vol.4, 1985, p.333.
3. G.N.Flerov, G.M.Ter-Akopian - Rep. Prog. Phys., 1983, 46, p.8I7.
4. G.M.Arzumanian et al., JINR, P7-81-744, Dubna, 1981.
5. G.M.Arzumanian et al., JINR, P7-82-552, Dubna, 1982.
6. G.M.Arzumanian et al., - J.Mass Spectrom.Ion Processes, 64 (1985), 255-264.
7. S.V.Stepantsov, A.M.Rodin and G.M.Ter-Akopian, JINR, P13-88-153, Dubna, 1988.
8. D.D.Bogdanov et al., JINR, P7-88-596, Dubna, 1988.
9. K.L.Brown, B.K.Klar and W.K.Howny, SLAC Report No.91, Stanford Linear Accelerator Center, Stanford, 1970.
10. J.Camplan, R.Meunier - Nucl.Instr. and Meth., 1981, 186, p.445.

Received by Publishing Department
on September 27, 1989.